Memoirs of the Kakioka Magnetic Observatory Vol. 16 No. 2 1975

Conductivity Anomalies in the Eastern Part of Hokkaido, Japan

Toshio MORI

Abstract

Field observations of geomagnetic and geoelectric variations were made at several stations in the eastern part of Hokkaido.

From the records, geomagnetic and geoelectric bay, si, ssc and similar short period variations are selected, and coefficients of preferred plain in which geomagnetic variation vectors lie, relations between geomagnetic horizontal vectors at Memambetsu Magnetic Observatory and those at the other temporary stations are studied. And at four stations, transfer functions are obtained from Fourier transforms of some isolated short events.

From model calculations of magnetic fields caused by current flowing in the deposits of Konsen Plain, it is confirmed that the deposits play an important role for the observed geomagnetic variations.

1. Introduction

Observations of geomagnetic and geoelectric variations were made at thirteen temporary stations in the eastern part of Hokkaido, Japan from 1970 to 1974. Locations of the stations are shown on the geological map in Fig. 1.

MO, SA, MT and HM are situated in green tuff region, AK and MI in Kuril volcanic chain, and the other stations in Konsen Plain. The region of south-eastern edge of Konsen Plain which lies to the east of HO along the coast of the Pacific Ocean is covered by Palaeogene and Cretaceous deposits (madstone, sandstone, tuff etc.) with spots of dolerites exposure. Other regions of Konsen Plain are covered by Quaternary and Neogene thick deposits.

Some results of the field observations made till 1973 have been reported by the present author[1], including Parkinson vectors and relations between horizontal vectors of geomagnetic and geoelectric variations. In 1974, three components of geomagnetic variations were observed by GIT-magnetometer of flux-gate type at SA in June, and at MO in July, and at SH from August to September. For the last period from August to September geomagnetic vertical component were observed by flux-gate magnetometer at AK, and geoelectric two components were observed at SH simultaneously. The span of electrodes for measuring the earth potential is 100 meters for both of NS and EW components.

Observations at SA and MO were carried out to confirm the Parkinson vectors were obtained from variations of total geomagnetic field at coastal stations of the Okhotsk Sea by S. Oshima and T. Mori[2].

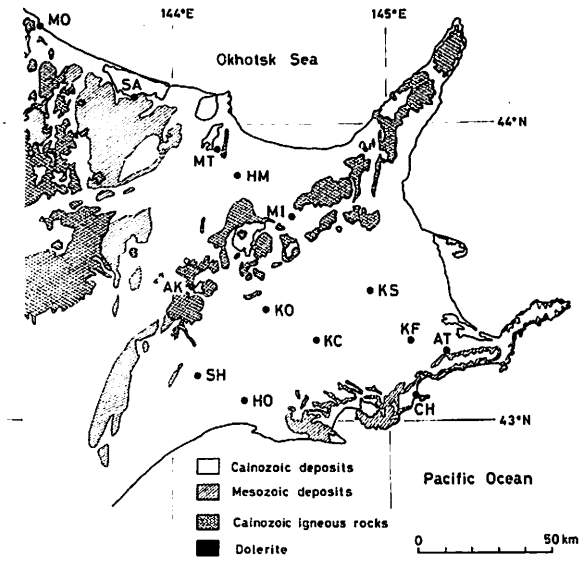

Fig. 1. Locations of geomagnetic and geoelectric observation points and geological map of the eastern part of Hokkaido. MT=Memambetsu Magnetic Observatory, MO=Mombetsu, SA=Saroma, HM=Higashimokoto, MI=Midori, AK=Akanko, KS=Kamishunbetsu, KO=Kamiosobetsu, KC=Kamichanbetsu, KF=Kamifuren, AT=Attoko, SH=Shitakara, HO=Hokuto, CH=Chanai.

2. Parkinson vector

It has been well-known that the vertical component ΔZ of short period geomagnetic changes is usually related to north and east components, ΔH and ΔD, by a relation

$$\Delta Z = A' \cdot \Delta H + B' \cdot \Delta D \,.$$

The coefficients of this equation have been usually expressed by A and B, but A' and B' are used here for A and B, respectively, to distinguish them from transfer function as described later. Parkinson vector is one of the expression of this equation.

Reading the amplitude of three components of bay, si, ssc and similar variations from the magnetograms at MO, SA and SH, A' and B' determined by least square method. As Z-component only observed at AK, A' and B' of the site are calculated by ΔZ at AK and ΔH and ΔD at MT. These A' and B' are shown in Table 1, and Parkinson vectors are shown in Fig. 2 together with those at HM, KO HO, KC, CH, AT and NA (Nakashibetsu) obtained by T. Mori[1),3)], that at MT by T. Kuboki and H. Oshima[4)], that at NE (Nemuro) by T. Kuboki[5)], that at WA (Wakkanai) by R. Maeda[6)] and those at MA (Mombetsu air port), ES

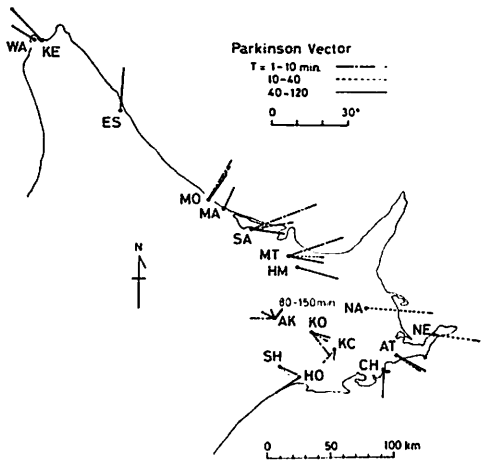

Fig. 2. Parkinson vectors in the northern and eastern part of Hokkaido.

(Esashi) and KE (Koetoi) obtained by using variations of geomagnetic total intensity by S. Oshima and T. Mori[2] in the northern and eastern part of Hokkaido.

Parkinson vectors in the northern and eastern part of Hokkaido are less than 0.5. The vectors point nearly to the east on the line which connects MT and NE, but the vectors in the south-western part of the region change remarkably from place to place. In particular, the direction of the vector at AK in Akan Caldera changes markedly according to change of period. The vectors at the coastal stations of the Okohtsk Sea gradually tend towards east to north-west as the station goes away towards WA from MT.

3. Transfer function

In the case that there are phase differences among H-, D- and Z-components, A and B are expressed by complex functions,

$$A = A_u + i \cdot A_v$$
$$B = B_u + i \cdot B_v ,$$

which are called transfer function.

Transfer functions can be obtained from Fourier transforms of some isolated short events or from power spectra of geomagnetic storms. J. E. Everett and R. D. Hyndman[7] have analyzed conductivity structure in south-western Australia using these two methods.

In this paper, the method of Fourier transform of short events is used.

Let variation $f(t)$ of a geomagnetic change of short duration be deviations from a straight line which connects beginning and ending of short event on magnetogram. Its Fourier transform is then computed as

Table 1. Relations among variations of geomagnetic three components and those between geomagnetic vector and earth-current vector in the eastern part of Hokkaido.

Station	Lat. (N)	Long. (E)	Duration time (min.)	$\Delta Z = A' \cdot \Delta H + B' \cdot \Delta D$				$\begin{pmatrix} E_x \\ E_y \end{pmatrix} = \begin{pmatrix} a & b \\ c & d \end{pmatrix} \cdot \begin{pmatrix} H_{0x} \\ H_{0y} \end{pmatrix}$			
				A'	B'	$\tan^{-1}\{(-B')/(-A')\}$	$\tan^{-1}\sqrt{A'^2+B'^2}$	a	b	c	d
Mombetsu (MO)	44°20′	143°22′	4—10	−0.26	−0.21	N 39° E	18°				
			10—40	−0.20	−0.17	N 41° E	15°				
			40—80	−0.16	−0.15	N 43° E	12°				
Saroma (SA)	44°06′	143°51′	4—10	−0.13	−0.51	N 76° E	28°				
			10—40	−0.01	−0.30	N 88° E	17°				
			40—100	0.06	−0.23	S 75° E	13°				
Akanko (AK)	43°27′	144°03′	4—10	−0.03	0.18	N 80° W	10°				
			10—40	−0.06	0.09	N 56° W	6°				
			40—80	−0.07	0.02	N 16° W	4°				
			80—150	−0.06	−0.06	N 45° E	5°				
Shitakara (SH)	43°09′	144°07°	4—10	0.07	−0.07	S 45° E	5°	0.32	1.38	−0.09	0.70
			10—40	0.07	−0.07	S 45° E	5°	0.40	1.08	0.05	0.53
			40—120	0.07	−0.12	S 60° E	8°	0.29	0.88	0.01	0.36

$$F(\omega)=\int_{-\infty}^{\infty} f(t)e^{-i\omega t}dt$$
$$\int_{t_0}^{t_n} f(t)e^{-i\omega t}dt$$

where $f(t)=0$ in $t\leqq t_0$ and $t\geqq t_n$. For some periods ($\tau=2\pi/\omega$), Fourier transforms of the three components (H, D, Z) are calculated, and A and B are determined to be the best fit for equation $Z=A\cdot H+B\cdot D$. Expressing the residual by

$$\delta_i = Z_i - A\cdot H_i - B\cdot D_i$$

for i-th event, the best fit is obtained by minimizing the value of sum,

$$\sum_{i=1}^{n} |\delta_i\bar{\delta}_i| = \sum_{i=1}^{n} (Z_i - A\cdot H_i - B\cdot D_i)(\bar{Z}_i - A\cdot\bar{H}_i - B\cdot\bar{D}_i)$$

Therefore A and B are given by,

$$A=\frac{\sum D_i\bar{D}_i\cdot\sum \bar{H}_iZ_i - \sum \bar{H}_iD_i\cdot\sum \bar{D}_iZ_i}{\sum H_i\bar{H}_i\cdot\sum D_i\bar{D}_i - \sum H_i\bar{D}_i\cdot\sum \bar{H}_iD_i}$$
$$B=\frac{\sum H_i\bar{H}_i\cdot\sum \bar{D}_iZ_i - \sum H_i\bar{D}_i\cdot\sum \bar{H}_iZ_i}{\sum H_i\bar{H}_i\cdot\sum D_i\bar{D}_i - \sum H_i\bar{D}_i\cdot\sum \bar{H}_iD_i}$$

Transfer function at MT, KO, KC and AT are calculated. Form the magnetograms at each station, ten events having predominant periods between 60 and 100 minutes are selected and transfer functions are calculated from readings in sampling interval of 5 minutes. The duration of these events are in the range of 110 to 230 minutes. Similarly for six or seven events whose predominant period are between 10 to 20 minutes transfer functions are obtained from sampling intervals of 1 minute. The duration is in the range of 20 to 60 minutes. The calculated transfer functions at MT, KO, KC and AT are shown in Figs. 3(1) to 3(4).

In these figures, A' and B', which has been obtained by the method of maximum range reading of short events by T. Mori[1] and T. Kuboki and H. Oshima[4], are shown too. A' and B' are approximately same as A_u and B_u, respectively, except B_u at AT for periods of 10-40 minutes. In the case that transfer function changes markedly according to change of period, the present author supposes that the method of maximum range reading will not give right period.

4. Earth-current

In 1974 observations of geoelectric variations were carried out at SH with simultaneous observation of geomagnetic variations. But till 1973 geoelectric observations were carried out at three temporary stations without simultaneous geomagnetic observations at the same stations. In the previous paper[1], relations between geomagnetic horizontal vector and earth-current vector have been studied by using geomagnetic data at MT and geoelectric data at the observed stations. This is also convenient for standardization of the relation when the difference of magnetic field is considered. So in the present paper also, geomagnetic data at MT is used instead of these at

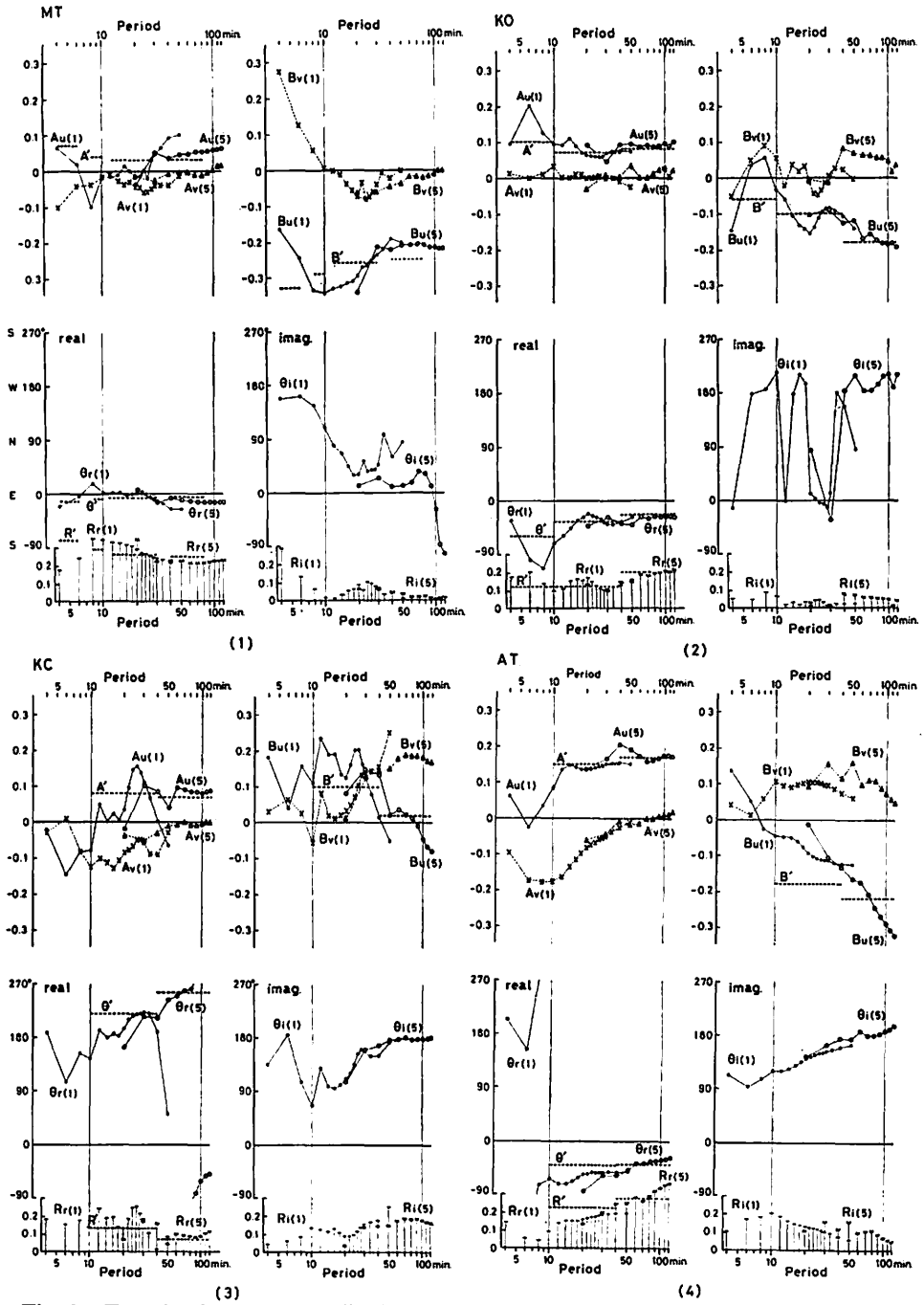

Fig. 3. Transfer functions; amplitude and direction of real and imaginary part. (1): sampling interval of 1 minute, (5): sampling interval of 5 minutes, $\theta_r=\tan^{-1}\{(-A_u)/(-B_u)\}$, $\theta_i=\tan^{-1}\{(-A_v)/(-B_v)\}$, $R_r=\sqrt{A_u^2+B_u^2}$, $R_i=\sqrt{A_v^2+B_v^2}$, $\theta'=\tan^{-1}\{(-A')/(-B')\}$, $R'=\sqrt{A'^2+B'^2}$.

SH to obtain the relation for SH.

Let geographic north and east components of geomagnetic variation at MT be H_{ox} and H_{oy} and those of earth-current variation at SH be E_x and E_y. Amplitudes and directions of the geomagnetic and the earth-current horizontal vectors are given by

$$H_0 = \sqrt{H_{0x}^2 + H_{0y}^2}$$
$$\theta_H = \tan^{-1}\{(-H_{0x})/(-H_{0y})\}$$
$$E = \sqrt{E_x^2 + E_y^2}$$
$$\theta_E = \tan^{-1}\{(-E_x)/(-E_y)\}$$

where θ_H and θ_E are direction angles measured counterclockwise from east for geomagnetic and earth-current vectors, respectively.

Fig. 4 shows changes of θ_E and E/H_0 at SH according to change of at MT. These relations may be expressed by

$$\begin{pmatrix} E_x \\ E_y \end{pmatrix} = \begin{pmatrix} a & b \\ c & d \end{pmatrix} \begin{pmatrix} H_{0x} \\ H_{0y} \end{pmatrix}$$

The coefficients a, b, c and d are determined by least square method. These coefficients are shown in Table 1. Fig. 5 shows earth-current vectors when θ_H at MT is 0°, 45°, 90° and 135° respectively in the case of the duration of 40-120 minutes in the eastern part of Hokkaido, where the vectors at the stations other than SH are those obtained previously by the present author[1].

At AT and CH, which are in the area of high positive Bouguer anomaly, E/H_0 are very large (3-5 mV/km/γ) and the directions are very steady at right angle to

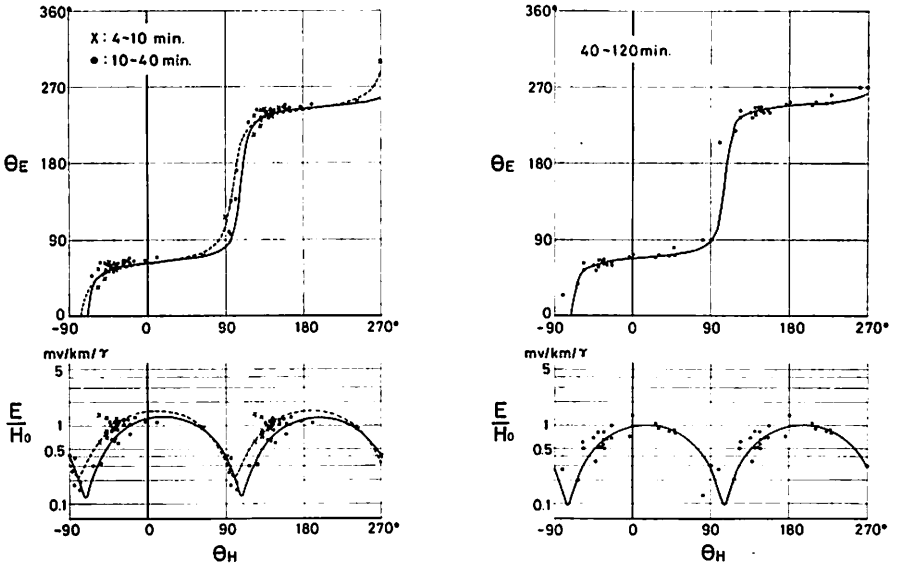

Fig. 4. Relation between geomagnetic vector at MT and corresponding earth-current vector at SH.

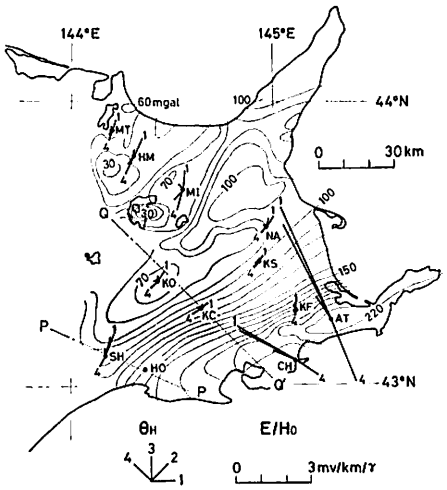

Fig. 5. Earth-current vector corresponding to geomagnetic vector of 1 (E), 2(N 45° E), 3(N) or 4(N 45° W), and distribution of Bouguer anomaly in mgal.

the coast line. On the other hand, at KO, KC, NA and KS located in the region of thick deposits, E/H_o are small (0.3-0.5 mV/km/γ) and the directions are not so steady, and those for maximum amplitude point nearly to the direction of the isodepth line of the deposits estimated by the present author[8].

5. Regional differences in horizontal vector of geomagnetic variation

Relations between horizontal vector of geomagnetic variation at MT and that at each other station are studied. Fig. 6 shows amplitude ratio for the horizontal vector at temporary stations to that at MT and differences of the direction at the stations from that at MT. The abscissa of these figures in the direction of the horizontal change at MT measured counterclockwise from geographical east.

At ST and HM near MT, the amplitude ratios and the directions do not change remarkably according to the change of the direction at MT. In Konsen Plain, the amplitude ratios at SH and HO change very markedly in the range of 0.8 to 1.3 and the ranges of the directional shifts amount to 30°, but those at KO and AT do not so largely.

As to means of the amplitude ratios, the means are smaller than 1 except the mean for the duration time of 40-120 minutes at SH.

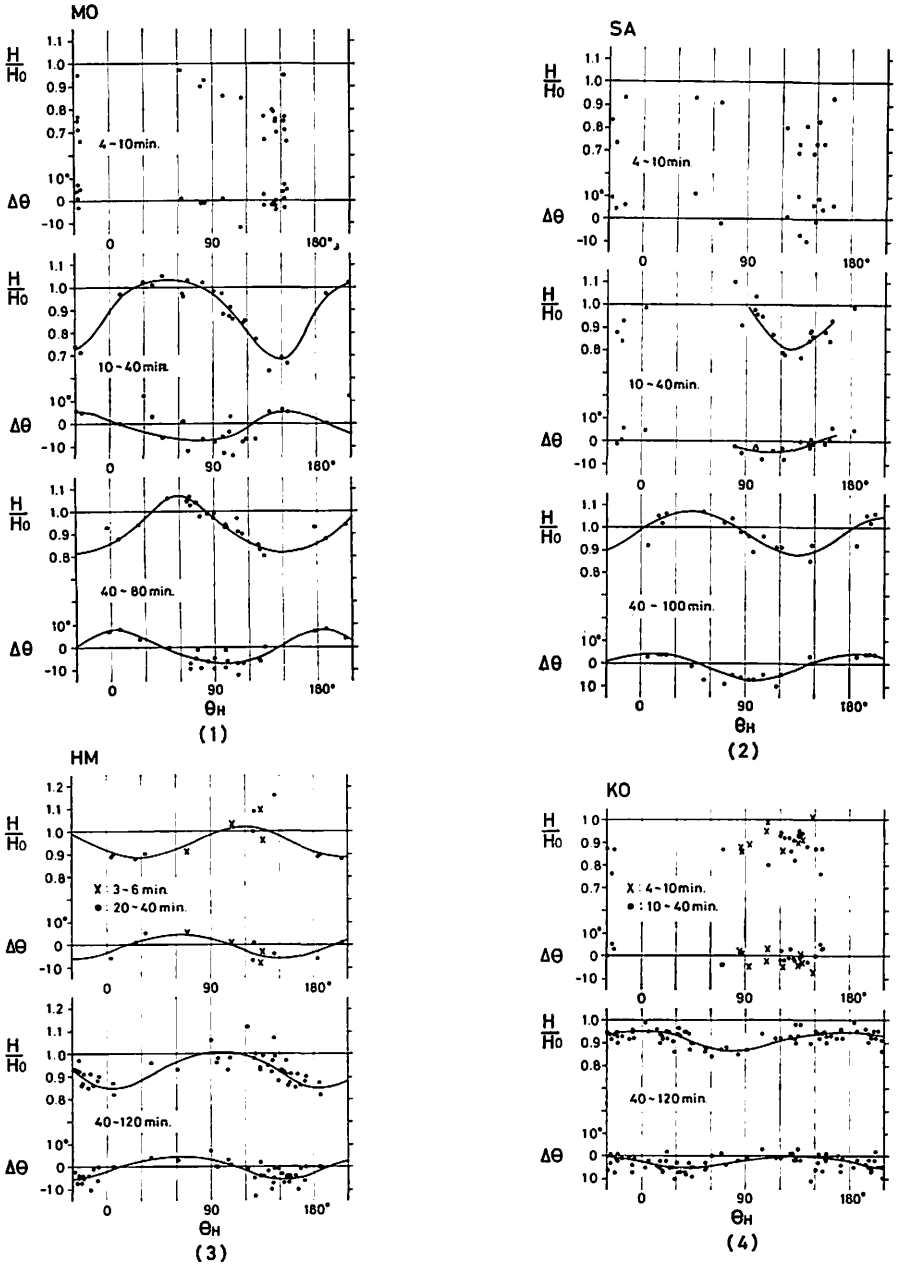

Fig. 6. Amplitude ratio and directional shift of geomagnetic horizontal vector at the temporary station for those at MT.

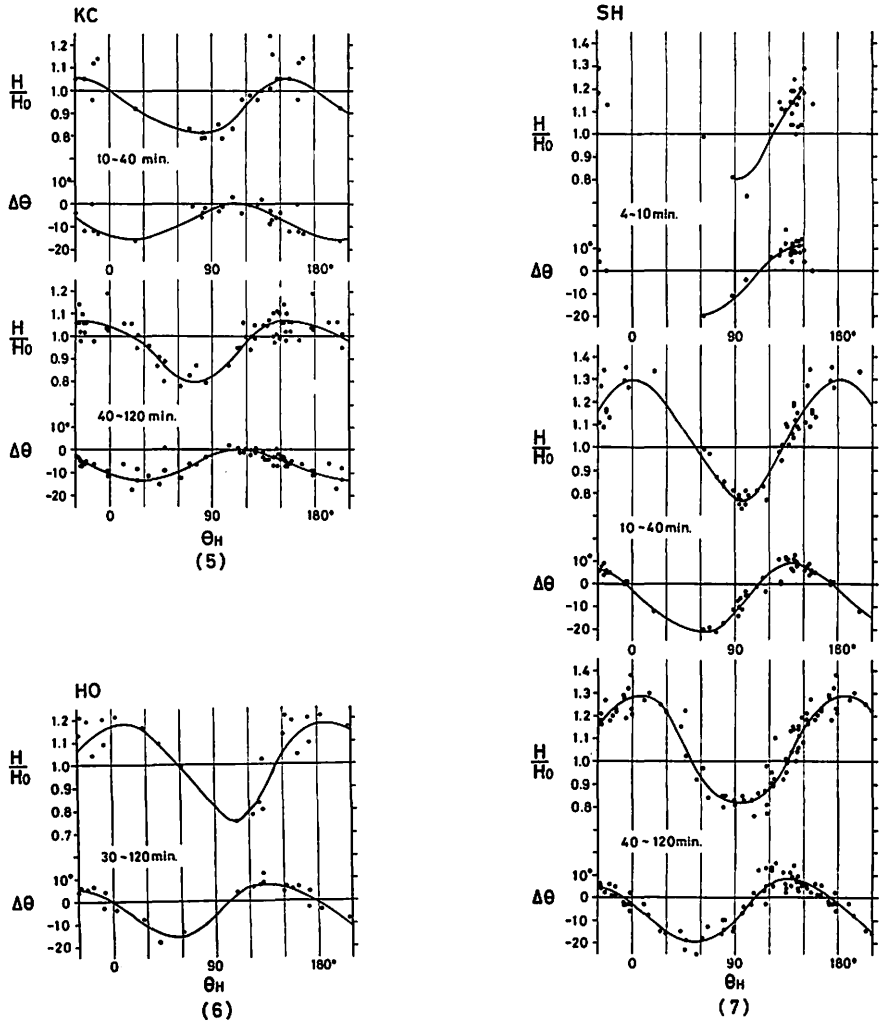

Fig. 6. Amplitude ratio and directional shift of geomagnetic horizontal vector at the temporary station for those at MT.

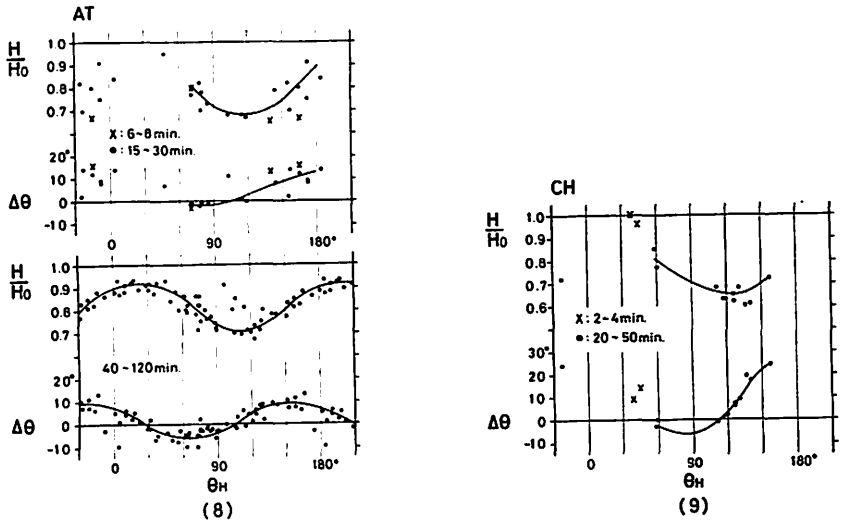

Fig. 6. Amplitude ratio and directional shift of geomagnetic horizontal vector at the temporary station for those at MT.

6. Effect of deposit

The present author[8] has discussed the crustal structure in the eastern part of Hokkaido and estimated the thickness of Cainozoic deposits at about 1.5 km and the depth of igneous rocks at 1.9 km at the shallowest in the middle of Konsen Plain. K. Yanagihara[9] has reported that amplitudes of geomagnetic short period variation changed remarkably according to location of observed station in Kanto district and these changes of observed fields might be explained by sedimentary layer. Similarly, supposing that the observed geomagnetic and geoelectric variations in Konsen Plain are affected by Cainozoic and Mesozoic deposits, effects of the deposits are discussed in this chapter.

The vector direction of electric field (earth-current) θ_E at SH is nearly constant for a wider range of magnetic field vector θ_H, as shown in Fig. 4. For example, when θ_E changes from –42° to 78°, θ_E does only from 56° to 76°. The mean θ_E for this range, which corresponds to the maximum value of E/H_o, is 66° (or 246°), which agrees well with the direction of the isodepth line of the deposits expected from Bouguer anomaly. The relation between geomagnetic horizontal vector at MT and earth-current vector at SH for the duration time from 10 to 40 minutes is given by

$$\begin{pmatrix} E_x \\ E_y \end{pmatrix} = \begin{pmatrix} 0.40 & 1.08 \\ 0.05 & 0.53 \end{pmatrix} \begin{pmatrix} H_{ox} \\ H_{oy} \end{pmatrix}$$

as seen in Table 1.

These tendency are also recognized in the case at KO, KC and NA in Konsen

Plain. The relation between geomagnetic horizontal vector at MT and earth-current vector at KC for the duration time from 10 to 40 minutes is given by

$$\begin{pmatrix} E_x \\ E_y \end{pmatrix} = \begin{pmatrix} 0.07 & 0.40 \\ -0.09 & 0.40 \end{pmatrix} \begin{pmatrix} H_{0x} \\ H_{0y} \end{pmatrix}$$

as obtained previously by the present author[1]. The θ_E at maximum E/H_0 is 45° (or 225°).

Profiles of the deposit are supposed along line P-P′ and Q-Q′ of Fig. 5, as shown in Figs. 7(1) and 7(2), respectively. The directions of the lines P-P′ and Q-Q′ are taken to be perpendicular to the preferred θ_E's which are the directions of maximum E/H_0 at SH and at KC, respectively. Resistivity (ρ) of the deposit is supposed to be very small in comparison with that of surrounding igneous rocks. Considering that the deposit is not so thick at MT, magnetic field of MT, which is used to study the relation between geomagnetic and geoelectric variations, is not so much influenced by deposits for the duration time from 10 to 40 minutes. Effect of deposits appears only in electric fields as far as the equation of the relation between geomagnetic and geoelectric variations concerns. We calculate magnetic fields produced by two-dimensional currents flowing in the conductive deposits which extend to infinity in the direction perpendicular to the profiles because the other currents parallel to the profiles are small as is deduced from the fact that the minimum to maximum ratio of E/H_0 is less than 10%. As to the resistivity of the deposits, the value of ρ=5

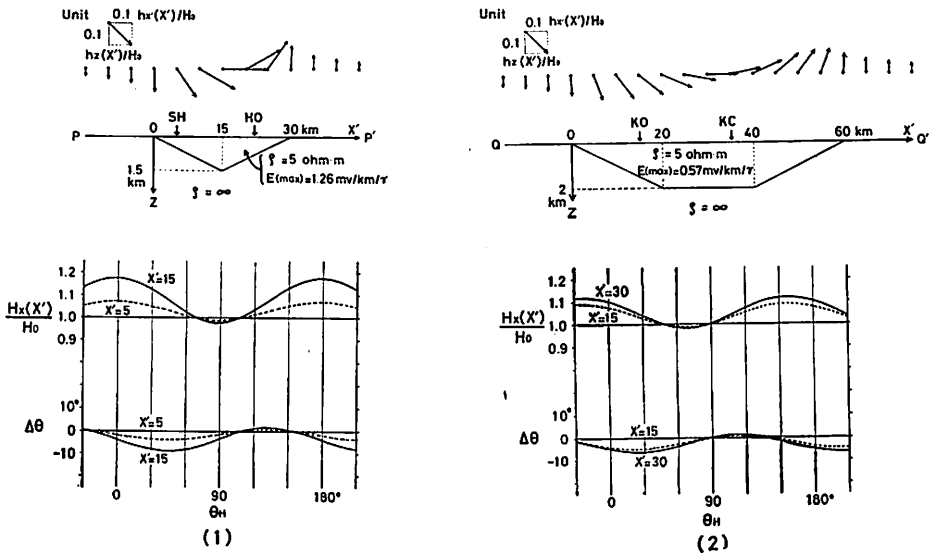

Fig. 7. Results of model calculation

Upper: magnetic field vectors on x'-axis caused by current in the deposits.

Middle: proposed deposit model.

Lower: amplitude ratio ($H_x(X')/H_0$) and directional shift ($\Delta\theta$) of magnetic horizontal vector at x'.

ohm·m are adopted because it seems to contain much water.

Let α be the angle taken counterclockwise from the geographical east to the line P-P′ or Q-Q′, and x'-axis be the line P-P′ or Q-Q′. The electric field perpendicular to x'-axis is given by

$$E' = \sqrt{E_x^2 + E_y^2} \cdot \sin(\theta_E - \alpha)$$

x'- and z-components of magnetic field at $(X', 0)$ on the x'-z plane are calculated by Biot-Savart's low,

$$h_x'(X') = \frac{E'}{5\rho} \iint \frac{z}{(x' - X')^2 + z^2} dx'dz$$
$$h_z(X') = \frac{E'}{5\rho} \iint \frac{x' - X'}{(x' - X')^2 + z^2} dx'dz$$

where $h_x'(X')$ and $h_z(X')$ are expressed in gamma, E' in mV/km, ρ in ohm·m, and x', X' and z in km. North and east components of sum of normal and additional magnetic fields are expressed by

$$H_x(X') = H_{0x} + h_x'(X') \cdot \sin\alpha$$
$$H_y(X') = H_{0y} - h_x'(X') \cdot \cos\alpha$$

For the normal field $\vec{H_o}$ (H_{ox}, H_{oy}), observed magnetic field at MT is used here. Consequently, amplitude ratio and directional shift of horizontal magnetic field at $(X', 0)$ on x'-axis for normal magnetic field are as following

$$\frac{H(X')}{H_0} = \frac{\sqrt{H_x^2(X') + H_y^2(X')}}{\sqrt{H_{0x}^2 + H_{0y}^2}}$$
$$\Delta\theta = \tan^{-1}[\{-H_x(X')\}/\{-H_y(X')\}] - \tan^{-1}\{(-H_{0x})/(-H_{0y})\}$$

The results of the calculation of the additional field $(h_x'(X')/H_o$ and $h_z(X')/H_o)$ vector, the amplitude ratio $(H(X')/H_o)$ and the directional shift $(\Delta\theta)$ on the line P-P′ and Q-Q′ are shown in Fig. 7(1) and Fig. 7(2).

Comparing the calculated amplitude ratios and the directional shifts of Fig. 7(1) with the observed ones shown in Fig. 6(7) (at SH) and Fig. 6(6) (at HO), it is found that the phases of these variations are very similar. However, the calculated amplitudes of the variations in the case of $X'=15$, where those becomes maximum, are less than a half of the observed ones at SH or HO.

There are KO and KC on the line Q-Q′ in Fig. 7(2). The amplitudes and phases of $H(X')/H_o$ and $\Delta\theta$ variations at $X'=15$ agree very well with the ones at KO shown in Fig. 6(4), but the amplitudes at $X'=30$, where those becomes maximum, are also less than a half of the observed ones at KC shown in Fig. 6(5). Consequently, in order to explain the observed geomagnetic fields from the deposits in Konsen Plain, it is necessary to enlarge the area of the cross section of the deposit or to introduce more conductive deposits.

Comparing the mean values of the amplitude ratio $(H(X')/H_o)$ in Figs. 7(1) and 7(2) with observed ones shown in Figs. 6(4) to 6(7), the formers are larger than

the latters. As this result can not be explained by the present deposit model, it is necessary to find out the other causes.

Arrows in the upper parts of Figs. 7(1) and 7(2) show the distribution of magnetic field vector along the lines P-P′ and Q-Q′ caused by the current in the deposit for the case of the maximum electric field. Calculated vertical components of the additional magnetic field are comparable with or larger than the observed ones except the center region of maximum depth. Therefore Parkinson vectors at SH, HO, KO and KC change remarkably if the influence of the deposits is taken away.

7. Discussion

Distribution of Parkinson vector, regional characteristics of earth-current and magnetic horizontal vector in the eastern part of Hokkaido are made almost clear.

Transfer functions at MT, KO, KC and AT are obtained by the method of Fourier transform of isolated short events. But as the isolated events which have predominant periods between 60 and 100 minutes and between 10 and 20 minutes are selected, the obtained transfer functions are inacculate for the period which is shorter than 10 minutes and between 20 and 60 minutes. Characteristics of period dependency of transfer functions at the observed stations will be discussed including present results in next paper.

In order to explain the observed geomagnetic field variation in Konsen Plain, the deposit models having the maximum thickness of 2 km are proposed, and the magnetic fields caused by the earth-current in the deposits are calculated using the relations between geomagnetic horizontal vector and earth-current vector obtained by the field observations. The amplitude ratios and the directional shifts of geomagnetic horizontal vector at the stations in Konsen Plain change according to the direction change of the magnetic vector at MT. The observed phases of the variations of amplitude ratios and directional shifts are well explained by the models, but the observed amplitudes of those variations aren't. The latters are about two times as large as the calculated ones. More suitable deposit model may explain this discrepancy. Any other source is not found yet. Anyway, it is confirmed that the effect of Cainozoic and Mesozoic deposits of geomagnetic field variations are very strong.

Meanwhile, it is an important problem that the amplitudes of geomagnetic horizontal vectors at MT are larger on the average than those at the other stations. T. Rikitake[10] has showed observed amplitude ratios of horizontal magnetic variation at ten Japanese observatories to that at Kakioka Magnetic Observatory. According to his study, the amplitude ratio at MT is 1.49, and this value is especially large in comparison with the others. It is considered that this is caused by leakage currents in the ionosphere from the auroral zone as his suggestion.[10] But considering that variations of horizontal magnetic field at MT are large compared with those at near stations in the eastern part of Hokkaido, it is necessary to search another cause for the increase at MT.

Acknowledgments. The writer would like to acknowledge the continuing guid-

ance and helpful advice of Dr. K. Yanagihara, Director of Kakioka Magnetic Observatory and Prof. I. Yokoyama of Hokkaido University. The writer also would like to express his sincere thanks to Mr. Y. Yamaguchi, Director of Memambetsu Magnetic Observatory, and his members who helped him in field observations. The writer's sincere thanks are also due to Dr. M. Aota of Hokkaido University who helped him in observation at Mombetsu.

References

1) T. Mori (1974); Observations of Geomagnetic and Geoelectric Variations in the Eastern Part of Hokkaido, Mem. Kakioka Mag. Obs., Vol. 16, No. 1, 45–58.
2) S. Oshima and T. Mori (1974); Geomagnetic Total Intensity Observation by Proton Magnetometer on the Geomagnetic Repeat Stations of Hydrographic Office, J. Geod. Soc. Japan, Vol. 20, No. 1–2, 70–76.
3) T. Mori (1968); On the Characteristics of Rapid Geomagnetic and Geoelectric variations in Hokkaido, Japan, Geophys. Bull. Hokkaido Univ., Vol. 20, 37–49.
4) T. Kuboki and H. Oshima (1966); The Anomaly of Geomagnetic Variation in Japan (Part III), Mem. Kakioka Mag. Obs., Vol. 12, No. 2, 127–198.
5) T. Kuboki (1927); The Anomaly of Geomagnetic Variation in Japan (Part IV), Mem. Kakioka Mag. Obs., Vol. 14, No. 2, 93–105.
6) R. Maeda (1969); Underground electric structure inferred from rapid geomagnetic variations, J. Radio Res. Lab., Vol. 16, 117–129.
7) J. E. Everett and R. D. Hyndman (1967); Geomagnetic variations and electrical conductivity structure in south-western Australia, Phys. Earth Planet. Interiors 1, 24–34.
8) T. Mori (1965); Gravity Anomalies in the Konsen Plain, Geophys. Bull. Hokkaido Univ., Vol. 14, 59–71.
9) K. Yanagihara (1971); Magnetic Field caused by Earth Surface Currents in Kanto District, Mem. Kakioka Mag. Obs., Vol. 14, No. 2, 79–87.
10) T. Rikitake (1965); Some Characteristics of Geomagnetic Variation Anomaly in Japan, J. Geomag. Geoelec., Vol. 17, No. 1, 95–97.

北海道東部の地下電気伝導度異常

森　　俊　雄

概　　要

1970年から1974年にかけて北海道東部で行った地磁気，地電流の観測結果を整理し，堆積層の効果について考察した。1973年までの観測結果の一部はすでに報告しているが，北海道東部およびオホーック海岸に沿ったパーキンソンベクトルの分布がほぼ明らかになった。女満別における地磁気変化の水平ベクトルと他の地点とのそれを比較した結果堆積層の厚いと思われる根釧原野の観測点と女満別との間に，地磁気変化の方向によって振巾比及び変化方向が大きく変ることが確かめられた。地磁気変化の方向によって振巾比及び変化方向が異る事は堆積層の存在によりほぼ説明できるが女満別での水平ベクトルの変化が平均して他の地点よりも大きい事に関しては他の原因を考えなくてはならない。